

# MICRO STRUCTURES AND MECHANICAL PROPERTIES OF A356 ALUMINUM CASTING ALLOY

Tetsuya TAKAAI\*, Nobuaki OHNISHI\*\*, Yoshihiro NAKAYAMA\*,  
Masaaki KOGA\*\* and Alberto DIONISIO\*\*

\* Faculty of Engineering, Yamanashi University (Kofu, Japan)

\*\* Graduate Student of Yamanashi University (Kofu, Japan)

## Abstract

Mechanical properties of A356 aluminum casting alloy usable as wheels for passenger car applications were mainly studied in view of casting conditions, heat treatment and related micro structures. Fine eutectic structures of the A356 alloy specimens were obtained with respect to wide selection of the cooling rates and variations of heat treatment conditions. Resistance ratio measurements were made for confirmation of the extent of redissolution of the solutes in various solutioning temperature and time. Certain metabolic improvements of mechanical properties were discussed in view of the micro structures related to the modifications of heat treatment and regulations of the cooling rates in the casting process.

## Introductions

Recently, energy or weight savings have become very important economic and social problems to be seriously solved. A356 aluminum casting alloy has been extensively applied as high quality cast products for traffic vehicles, airplanes and structural materials for hydraulic pressure systems in point of weight or energy saving.

Improving the strength of the materials is considered to be one of the most effective measures for weight and energy savings. In the case of A356 casting alloy, various simple methods have been discussed by several authors [1,2,3,4,5] for effective improvements of the strengths as illustrated in Fig.1. The effect of regulations of the cooling rates on the eutectic regions of the cooling curves and related micro structures of A356 aluminum casting alloy have been extensively studied[6,7,8,9] in relation to the improvements of mechanical properties or toughness. However, the details of the mechanisms embracing the effect in modifications of the heat treatment conditions and the effect in regulations of cooling rate conditions are obscure. The present

study has been achieved with the intention of studying further the improvement of the strength or toughness of the A356 casting alloy and considering the detailed mechanism of modification in micro structures and related mechanical properties.

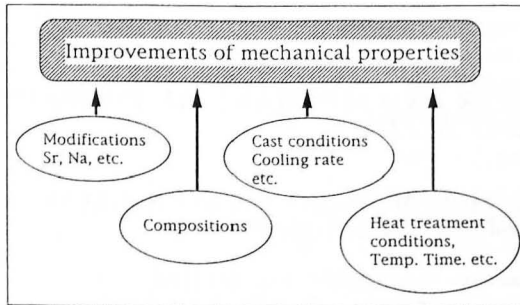


**Fig.1 Schematic illustration showing the improvement of the mechanical properties of the A356 casting alloy.**

### **Materials and procedures**

#### **Materials**

The A356 alloy specimen was modified by addition of strontium containing mother alloy and prepared mainly from the normal production runs and poured into a permanent mould. Chemical analysis results of the specimen are shown in Table 1.

**Table 1 Chemical composition of A356 casting alloy**

Elements	Si	Mg	Fe	Zn	Cu	Ti	Sr
mass %	7.06	0.32	0.11	0.02	0.02	0.11	76ppm

Size and shape of the tensile and Charpy impact test pieces applied in the present study were prepared in accordance with the specifications of the Japan Industrial Standard(JIS).

#### **Procedures**

Cooling rates while casting the A356 alloy were extensively controlled in the present study applying two casting methods. One of which is a regulation of the initial temperature of the permanent moulds and the other is a variation of the shape and size or gap of the permanent mould. In the case of the control of the initial mould temperatures, three heating temperatures were prepared, such as, 373, 573 and 773 K. In the latter case, four selections of the metallic mould gaps, 3, 6, 10 and 15 mm were made. The cooling rates  $dT/dt$ , were estimated for the former case as 5.0, 3.6 and 0.9  $Ks^{-1}$  respectively for the cooling temperatures ranging from 883 K(liquidus temperature of the A356 alloy) to 849.5 K( main eutectic temperature of the A

356 alloy) basing upon the data obtained by preliminarily achieved differential thermal analysis(DTA). According to DTA, Al-Si-Mg<sub>2</sub>Si ternary eutectic temperature of the present A356 alloy specimen was measured as 827.4 K. In the latter cooling method, the rates dT/dt were estimated as 12.1, 6.0, 4.1 and 3.3 Ks<sup>-1</sup> respectively for the temperatures ranging from 923 to 823 K in accordance with the temperature-time record obtained during casting. Thus, the present study was achieved for the above seven kinds of specimens, cast under extensively selected various cooling rates.

## Results and discussions

### Effect of cooling rates on dendritic growth

Pronounced refining effects of the cooling rate on the dendritic growth were attained for the specimens cast under the higher cooling rates of 12.1, 6.0 and 5.0 Ks<sup>-1</sup>. Mean secondary dendrite arm spacings(DAS) were plotted against the log cooling rates in Fig.2 for the respective cooling methods of the casting. Reasonable linear relations were obtained between the log mean values of the DAS and logarithm of the cooling rate dT/dt in accordance with the following simple equation (1) for each of the applied casting cases.

$$\text{Log } R = k \text{ Log } d + m \quad (1)$$

Where R: cooling rate dT/dt, d: mean value of the secondary arm spacing and k, m are constants.

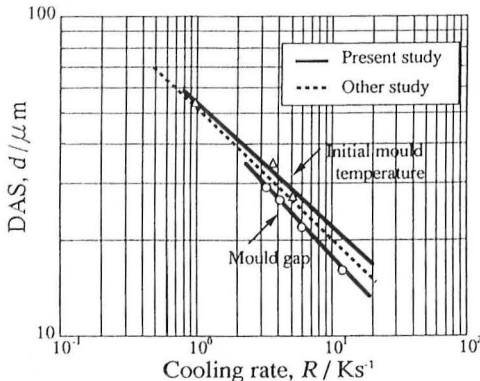


**Fig.2 Effect of cooling rate on dendrite arm spacings.**

Slight differences in value were observed for these constants of the different cooling procedures compared to those of the reference data -0.42 for m and 1.73 for k[5]. However, the differences were so insignificant that the obtained values of the constants were substantially comparable with the reference values in spite of the variations of the cooling modes of the casting.

### Solution treatment

Solution treatment of the A356 alloy specimens were achieved mainly at 843 K which was about 40 K higher than that of the ordinary solution treatment temperature. After the solution treatment at 843 K the dendritic micro structures showed clearly a characteristic growth as compared to those obtainable at the ordinary solution treatment temperature, however, no remarkable traces of the overlapped effect of the cooling rates were observed on the dendritic growth. With respect to the spheroidization coefficient of the specimen, solution treated at 843 K, an evident tendency of converging to a desirable high value near unity was confirmed.

It is clear from the measurement of the resistance ratio that the increase of the solutioning temperature is directly effective to the increase of the solutes in the matrix. However, the solutioning of the solutes seems to be saturated enough at 833 K for the solutioning time less than 1 min. It seemed that no extension of the solutioning time was necessary once the solutioning temperature of 843 K was reached.

It can be also easily estimated that solutioning of the solutes has been completed at 843 K before the specimen temperature reached to 843 K. With respect to the present solutioning treatment, about a 10 % improvement of tensile properties was attained as compared to those of ordinary solutioning temperature conditions[8]. In addition to the effect of the selection of high temperature solutioning on the mechanical properties, certain additional effects were secured in the present study by reasonable regulations of the cooling rates. Effects of solutioning temperature and time on the redissolution of the solutes and shape or size of the eutectic were shown together in Fig.3.

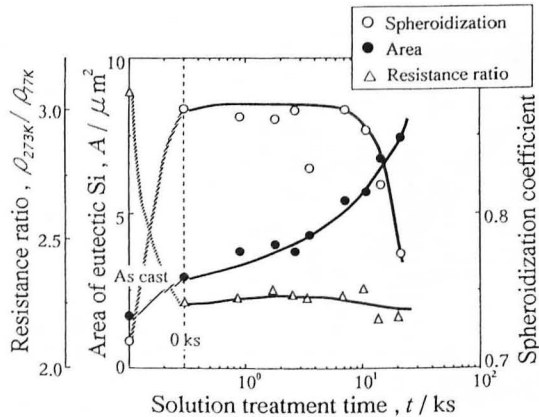


**Fig.3 Effect of solutioning temperature and time on the redissolution of the solutes, and shape or size of eutectic.**

Certain premium effect of the cooling rates on the tensile properties are considered to be due to effective spheroidization and refining or appropriate distribution of eutectic silicon as shown in Fig.3 against the solutioning time. It is clearly seen that an area ( $\mu\text{m}^2$ ) of eutectic silicon, which was refined

by higher casting rates, increases linearly as solutioning time increases. Substantially higher values near but below unity of the spheroidization coefficients were maintained at high temperature solution treatment of 843 K but independent of time until 8 Ks of solutioning time. Beyond about 10 Ks, however, spheroidization coefficients fell sharply probably due to cohesion or growth behaviors of the eutectics. In other words, size of eutectic silicon grows remarkably as the solutioning time increases beyond about 10 Ks in spite of suitable spheroidization coefficients under higher cooling rates. According to the change of the resistance ratio against logarithmic plot of solutioning time taking solutioning temperatures as parameters, the lowest resistance ratio was attained for the specimens solution treated at the highest temperature of 843 K. However, the measured resistance ratio was almost independent of solutioning time except certain confusion of the effect of the temperature. Therefore, the present author's reasonable selection of solutioning temperature and time are appreciated due to the improvements of the mechanical properties. It is clearly observed from the resistance ratio measurement and chemical analysis results that the extents of the redissolution of the solutes became higher as the cooling rate increased.

### Aging treatment

Effect of aging treatment on the resistance ratio  $\rho_{273K}/\rho_{77K}$  was studied for the specimens cast under various conditions of the cooling rates. The resistance ratio was measured for the specimens solution treated at 843 K and subsequently aged. As indicated in Fig.4, the resistance ratio increased in a parabolic manner as the aging time increased. Substantial further effects of the cooling rate on the resistance ratio was observed for the specimens of as cast conditions, however, no effect of the cooling rates was observed in the aging process and in the solution treated conditions of the respective specimens.

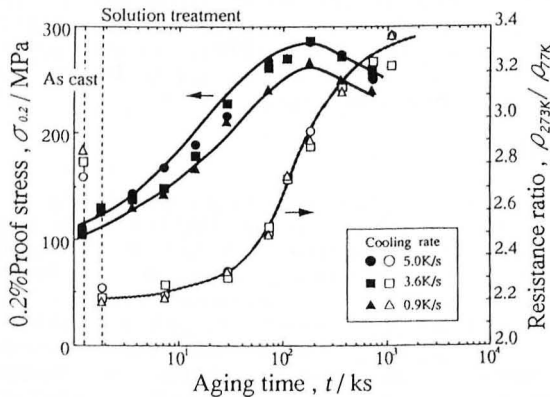


**Fig.4** Aging response of the resistance ratio and the proof stress for the specimens cast under various cooling rates.

Peak values of 0.2% proof stress existed at about  $2 \times 10^2$  ks aged at ordinary aging temperature of 423 K. Differences of about 20 MPa in 0.2 % proof stress were observed between the specimens cast under higher cooling rate of  $5.0 \text{ ks}^{-1}$  and the specimens cast under lower cooling rate of  $0.9 \text{ ks}^{-1}$ . In other words, effect of rapid cooling by the casting was overlapped by about 8 % additional improvement on the 0.2 % proof stress due to the high temperature solution treatment effect.

Aging response to 0.2 % proof stress of the A356 alloy specimens are shown together with the variation of the resistance ratio in Fig.4. The peak values of the proof stress were observed before the resistance ratio reached their maximum value.

Previous studies and measurement of the variations of the resistance ratios and 0.2 % proof stresses showed that the rate process of the aging of the A356 alloy specimens were determined reasonably by Johnson-Mehl's relations[5]. With respect to the Johnson-Mehl's plot, the exponent  $m$  value was estimated to be in the range of 0.9 to 1.3 and was classified into two groups in accordance with the aging temperature.

Differences in exponent  $m$  values are considered to be closely corresponding to the variation of characteristic shape and size of the precipitates[10]. A relatively lower value of the activation energy of 110-130 kJ/mol was calculated from the relations between the reaction rate constants and aging temperatures of the A356 alloy specimen.

### **Tensile properties**

Effects of the cooling rates were more clearly observed in the tensile strength than in the 0.2 % proof stress. Obtained tensile strengths were plotted in Fig.5 as a function of the aging time together with the absorbed energy of the Charpy impact fracture taking cooling rates as parameters. Differences or improvements of the tensile strength due to the variation of the cooling rates were estimated as about twice as compared to that of the proof stress at the peak value except certain deviations of the measured values were observed. In other words, tensile strengths were improved effectively further by appropriate selection of rapid cooling rates and were more sensitive to the cooling rates than the proof stress.

### **Charpy impact properties**

Charpy impact properties were investigated by measuring the absorbed energy during the Charpy impact fracture. Absorbed energy of the A356 alloy specimen is generally affected sensitively with the micro structures, above all, size and shape of the eutectic silicon phase. The absorbed energies were plotted against the aging time in Fig.5 together with the tensile strength cooling rates as parameters. Variations of the absorbed energy regarding the cooling rates were fundamentally the same with those of the tensile strength, however, the peak values of the energy were shifted to the early time of aging. The behaviors of the absorbed energy against the cooling rates and aging temperature or time were quite similar to those of the

elongations to fracture.

Differences of the absorbed energy due to the variation of the cooling rates were further increased as compared to those of the tensile strength and 0.2 % proof stress. This means that the absorbed energy is more sensitive to the micro structural change due to the variable regulations of the cooling rates.

Ordinary values of the absorbed energy obtainable by the usual heat treatment and cooling rate conditions are below  $10 \times 10^4 \text{ J/mm}^2$ , however, as shown in Fig.5 the peak values of the absorbed energy measured for the specimens cast under higher cooling rates were higher than  $15 \times 10^4 \text{ J/mm}^2$ .

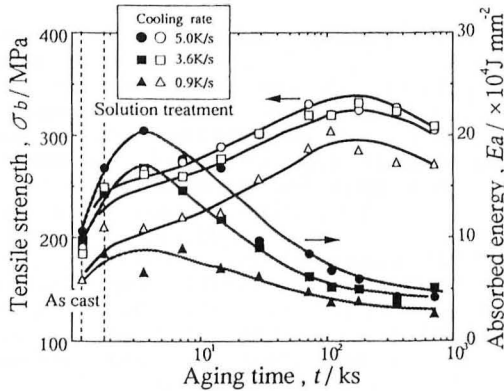


**Fig.5** Aging response of the tensile strength and Charpy impact properties of the A356 alloy specimens cast under various cooling rates.

One of the reason that the effect of the cooling rates improving the mechanical properties and absorbed energy is considered to be a change of magnesium concentration in the matrix phase. Magnesium concentrations in the matrix phase were plotted in Fig.6 with relation to the heat treatment and aging time taking the cooling rates as parameters. As known from the diagram, Mg concentrations in the matrix were variable extensively in accor-

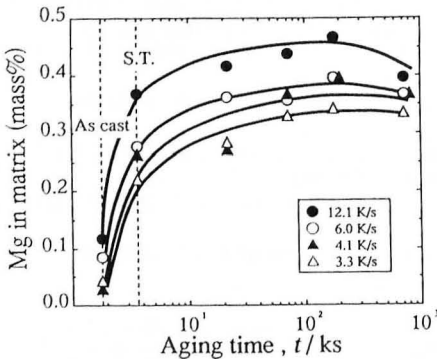


**Fig.6** Change of Mg concentrations in the matrix by various cooling rates.

dance with the heat treatment and aging process. Relatively higher concentrations were attained as the cooling rates were increased. Lower concentrations in as cast conditions are probably due to preferential segregations of magnesium atoms in the eutectic region. Remarkably high concentrations of Mg in the solution treated condition is probably due to the effective diffusion behaviors of magnesium atoms into the matrix. Mg concentrations increased generally as the aging treatment progressed and the highest values of Mg concentration were nearly correspondent to the peak values of the tensile properties.

### Conclusions

From the present experimental study, the following concluding remarks were obtained;(1) Redissolutions of the solutes were accelerated effectively as the solutioning temperature was increased. (2) No marked effect of the extension of the solutioning time on the extent of redissolution was observed at higher solutioning temperature. (3) Size and shape of the eutectic silicon phase were modified pronouncedly by regulations of the cooling rates and solutioning temperature and time. Above all, statistic size and spheroidization coefficients were changed by the high temperature solutioning and subsequent aging treatment. (4) Certain metabolic improvements of mechanical properties were secured by selecting higher solutioning temperature and faster casting cooling rates. (5) Tensile elongations to fracture and absorbed energies were improved a little by selection of high temperature solutioning, however, about 8 to 10 % improvements were attained by the increased cooling rates during casting. (6) Magnesium concentrations in the matrix increased with the lapse of aging time and the maximum value of the magnesium concentration were nearly correspondent to the peak value of the tensile properties.

### References

1. S.Tsuchida, H.Yoshida;Journal of Japan Inst. of Light Metals, 39(1989),587.
2. S. Fujiki, M.Tsukada; Journal of Japan Inst. of Light metals, 33(1983),712.
3. H.M.Tensi, R.Rosch and C.Xu;Proceedings for the 3rd Internat. Conf. on Aluminum Alloys, June 22-26,1992, Trondheim, 87-92.
4. M. Koga, T. Takaai, Y. Nakayama, N. Ohnishi; Journal of Japan Institute of Light Metals, 43(1993),297.
5. M.Koga, T.Takaai, Y.Nakayama et al;Journal of Japan Institute of Light Metals, 43(1993),612.
6. Methods of measuring the DAS and cooling rate; edited by Japan Institute of Light Metals(1988),Tokyo.
7. A. Kamio, H. Tezuka and T. Takahashi; Journal of Japan Inst. of Light Metals, 32(1982),124.
8. M.Koga,T.Takaai,Y.Nakayama, N.Ohnishi; Journal of Japan Inst. of Light Metals, 44(1994),216.
9. T.Takaai,Y. Nakayama, N.Ohnishi et al; Proceedings for the 32nd Conf. of Metallurgist of CIM, Aug.29-Sep.1(1993),535.
- 10.H.Sudoh; Kikai Zairyo, korona Publ. Ltd.,(1985),55 Tokyo